



PII: S0017-9310(97)00284-6

# Effective medium approximation for the conductivity of sensible heat in dry snow

EDWARD M. ARONS† and SAMUEL C. COLBECK

U.S. Army Cold Regions Research and Engineering Laboratory, 72 Lyme Rd, Hanover, NH 03755-1290, U.S.A.

(Received 9 August 1996 and in final form 18 September 1997)

**Abstract**—We developed an inductive model for thermal conductivity of sensible heat of deposited snow using random resistance network theory and parametric statistics. The model identifies the geometric quantities that determine this physical property. It allows us to quantitatively link conductivity to natural transformations that are known to change conductivity and increases our ability to test such theories experimentally. We are now able to show how microstructural quantities such as grain size distribution and average coordination number interact with each other to govern conductivity. These results may easily be extended to other porous geological and industrial materials. © 1998 Elsevier Science Ltd. All rights reserved.

## INTRODUCTION

Our understanding of the macroscopic physical properties of a wide range of geological materials is increasingly dependent on our ability to make sense of their microscopic structures. The composition of porous media varies with grain size distribution, connectivity, and degree of intergranular bonding [1, 2]. Thermal properties vary with compositional changes and these variations must be understood to estimate exchanges of mass and energy between snow covers and the atmosphere and hydrosphere. Sturm *et al.* [3] analyzed the long history of correlating snow thermal conductivity with density. Adams and Sato [4] modeled the conductivity of randomly packed ice spheres and demonstrated the importance of intergranular bonding for heat flow. Shabtaie and Bentley [5] used concepts from percolation theory to correlate microstructure and thermal conductivity of dense snow and firn. Kossacki *et al.* [6] used sintering theory and a simple packing scheme for ice spheres to demonstrate that bond growth in low density porous ice can cause sensible thermal conductivity in cometary materials to range over two orders of magnitude. In a theoretical investigation of mechanical properties, Watanabe [7] predicted the tensile strength of dry snow using a model that consisted of systematically arranged ice spheres with varying network connectivity and bond size.

We sought an inductive method for predicting thermal conductivity of snow based on specific microstructural properties that have physical meaning for heat transfer. To accomplish this, we used effective medium theory [8] to identify the fundamental par-

ameters that control heat flow through the ice grain lattice. We developed a model for thermal conductivity that can respond to the metamorphic processes in snow, whose physical causes are largely understood. This approach does not treat the contribution of latent heat transfer to snow thermal conductivity. The latent component arises from water vapor diffusion that is driven by temperature gradients. In the absence of convection, latent heat transfer may account for as much as 50% of the total heat transfer, depending on temperature and snow type. The latent heat transfer component also depends on microstructure, but this dependence is too complicated to be treated by the effective medium approximation at present.

## EFFECTIVE MEDIUM APPROXIMATION

The effective medium approximation (EMA) is an outgrowth of the more general percolation theory [8]. The type of approximation that applies most sensibly to snow is the lattice EMA. This approximation assumes that the material of interest can be modeled as a random lattice in which transport occurs in quasi-linear segments, which meet at junctions where the transported quantity is conserved [9]. The central concept is that macroscopic potential fields (e.g., temperature or voltage) are produced by the combination of a large number of microscopic fields surrounding individual conduction elements. At any location in the heterogeneous material, the field may be thought of as the sum of the microscopic field due to the nearest conductor and the macroscopic field due to the total effect of all the other conductors in the network. This sum and Fourier's equation are used to find an ensemble mean value that, when the conductances are

† Author to whom correspondence should be addressed.

## NOMENCLATURE

$A(z)$	cross-sectional area of intergranular bond	$m$	mass per water molecule
$A_p$	area of plane for calculation of $t$ -factor	$M$	slope of $g$ with respect to $r_{\text{grain}}$
$b$	intercept of $g(r_{\text{grain}})$	$p_0$	equilibrium water vapor pressure over a plane ice surface
$B(T)$	sintering diffusivity	$q$	heat flux due to conduction
$c$	distance in $z$ direction between center of intergranular bond and plane separating $R_1$ from $R_2$	$q_{\text{diff}}$	heat flux due to conduction and mass diffusion
$D_g$	diffusion coefficient of water vapor in air	$r_{\text{grain}}$	grain radius
$f(r_{\text{grain}})$	probability density function of grain radius	$R_1, R_2$	thermal resistance of region of intergranular bond
$g$	intergranular bond thermal conductance	$t$	time
$g_m$	ensemble mean thermal conductance	$T$	absolute temperature
$G(g)$	probability density function of conductance	$x$	intergranular bond radius
$I$	total number of bonds passing through $A_p$	$z$	displacement coordinate along intergranular bond.
$k_{\text{air}}$	thermal conductivity of air	<b>Greek symbols</b>	
$k_b$	Boltzmann's constant	$\gamma$	surface tension of ice/air interface
$k_{\text{ice}}$	thermal conductivity of ice	$\delta$	intermolecular spacing of water molecules in ice
$K_{\text{lat}}$	thermal conductivity of ice grain lattice	$\zeta$	coordination number
$K_{\text{total}}$	thermal conductivity due to conduction and mass diffusion	$\eta$	mean grain radius
$K_{\text{vap}}$	thermal conductivity due to mass diffusion	$\theta$	angular displacement of coordinate of $\rho$
$L_i$	length of $i$ th bond passing through $A_p$	$\rho$	outside radius of curvature of cylindrical walls in region $R_2$
$L_s$	specific latent heat of sublimation of water	$\rho_{\text{ice}}$	ice density
		$\rho_s$	snow density
		$\sigma$	standard deviation of grain radius
		$\phi_i$	angle between $i$ th bond and macroscopic temperature gradient.

assembled in a network, generates the correct macroscopic conductance [9, 10].

The approximation of the ice grain lattice thermal conductivity,  $K_{\text{lat}}$ , is given by

$$K_{\text{lat}} = g_m \cdot (t\text{-factor}) \quad (1)$$

in which  $g_m$  is the ensemble mean conductance value based on intergranular bond shapes, and the  $t$ -factor is a spatial average that is weighted with respect to conductor lengths and orientations.  $g_m$  is the solution of

$$\int_{-\infty}^{\infty} G(g) \frac{g - g_m}{\left(\frac{\zeta}{2} - 1\right)g_m + g} dg = 0 \quad (2)$$

in which  $g$  is the random variable representing intergranular bond conductance values,  $G$  is the probability density function of  $g$ , and  $\zeta$  is the mean coordination number (number of bonds per grain). The  $t$ -factor arises from the assumption of steady state flow and is given by

$$t\text{-factor} = \frac{1}{A_p} \sum_{i \in A_p} L_i \cos \phi_i \quad (3)$$

in which  $A_p$  is the area of a plane normal to the macroscopic temperature gradient through which a total of  $I$  bonds (conduction elements) pass.  $L_i$  is the length of the  $i$ th bond and  $\phi_i$  is the angle between the  $i$ th bond and the macroscopic temperature gradient [11].

Koplik [12] has demonstrated excellent agreement between this approximation and the numerical solution for a variety of standard networks (e.g., hexagonal, trigonal, cubic). However, Koplik *et al.* [11] attributed disagreement with sandstone results to insufficient sampling of laboratory samples, oversimplification of pore space geometry for modeling purposes, and relationships between pores that invalidated key assumptions about statistical independence of flow paths. Our theoretical application of EMA to snow is not limited by sample size, and we treat flow correlation explicitly to avoid similar problems. Nevertheless, we are forced to make geometric sim-

plications that impose limitations on the applicability of the method.

### APPLICATION OF EMA TO SNOW

Falling snow crystals occur in a variety of forms, but once snow is deposited on the ground, grains bond together and tend to become rounded. Atmospheric conditions accelerate geometric changes that are driven by thermodynamic instabilities (e.g. [13]). There is a continuous spectrum of metamorphic states of deposited snow, and the spectrum is so wide that it is useful to characterize the material based on grain size distribution, bulk density, and dominant metamorphic processes [14].

In most cases, the advective and radiative components of heat transfer can be neglected in snow. Then, the most convenient way to account for total diffusive thermal conductivity is to treat it as a sum of thermal conduction through the ice grain lattice and of the transfer of latent heat by water vapor diffusion. Conduction through air is ignored because it is two orders of magnitude smaller than that through the ice. Diffusive heat flux is then written as

$$q_{diff} = -K_{total} \nabla T = -(K_{lat} + K_{vap}) \nabla T \quad (4)$$

where  $K_{lat}$  is the thermal conductivity of the ice grain lattice and  $K_{vap}$  is the effective thermal conductivity that is associated with the transfer of latent heat of water vapor. The two mechanisms are typically modeled as parallel, but on the scale of grains, they are clearly hybrid parallel-serial pathways (e.g. [1]).

There have been direct measurements of  $K_{lat}$  by using low temperatures to suppress the effects of vapor transport [15–17], but we know too little about the microstructural conditions in the experiments that led to these values to be useful in determining the dependence of thermal conductivity on microstructure.

### MODEL REQUIREMENTS

We must define clearly the nature of the flow through the system to model the snow as a system of random thermal resistors (or conductors). Heat flow must follow Fourier's equation and it must be conserved at every point in the network [10]. The elements that we model as conduction elements in the network must be linear (or quasi-linear) and statistically independent. The first requirement arises because we assume that there is a constant angle  $\phi$  between an individual conductor and the macroscopic temperature gradient. In principle, tortuosity of individual conductors could be admitted by allowing  $\phi$  to vary along the length of the conductor and weighting the contribution of each conductance element accordingly. We assume that the conductance elements are the intergranular bonds that grow naturally between ice grains. If we further assume that an individual

conductor is a bond between the centroids of two spherical grains (Fig. 1), then the linearity requirement is met.

The second requirement calls for additional caution. If grains are connected in a systematic way, such as those in a chain, we must expect that flow through a grain in the middle of the chain would depend on flow through the end-members of the chain. Thus, flow through these grains would be statistically dependent. In contrast, some snow is generally isotropic and lacks obvious multigrain structures. In general, snow held at a constant temperature is much less likely to be dominated by multigrain structures than snow held under a temperature gradient. We assume that flow among grains of the former is statistically independent while flow among grains of the latter is not.

### MODELING THE CONDUCTORS IN SNOW

Intergranular bonds are approximately hourglass-shaped. As the bond develops, the bond diameter grows and the outside radius of curvature (Fig. 1) increases. Using the analogy between electrical and thermal resistance and summing incremental conductances ([18], p. 507), we calculate snow's conductance using

$$g = \lim_{\Delta z \rightarrow 0} \left[ \sum_i \frac{\Delta z_i}{k_{ice} A_i(z)} \right]^{-1} \quad (5)$$

where  $g$  is the effective bond conductance,  $k_{ice}$  is the conductivity of ice, and  $A_i(z)$  is the cross-sectional area (Fig. 2). This conductance is then used in the calculation of the conductance of the average conductance element,  $g_m$ .

We calculated the effective thermal conductivity of bonds between pairs of identical spherical grains in snow. It would be ideal to be able to treat the individual grains in each bonded pair as if their sizes were statistically independent, but our simplification is justified by Kuzczynski's [19] observation that bond growth is controlled by the smaller grain.

Our working definition of the bond is the ice between planes that intersect the grain centroids ( $z_1$  and  $z_2$  in Fig. 2). Using equation (5), we summed the series of incremental thermal resistances instead of conductances along the bond axis for the spherical and paraboloid regions. This gives the thermal resistance of Region I (Fig. 1):

$$R_1 = \frac{1}{k_{ice} \pi r_{grain}} \tanh^{-1} \left( \frac{r_{grain} - c}{c} \right) \quad (6)$$

where  $r_{grain}$  is grain radius, and  $c$  is the length in the  $z$ -direction between the intersection of the two regions and the center of the bond. The resistance of Region II is given by

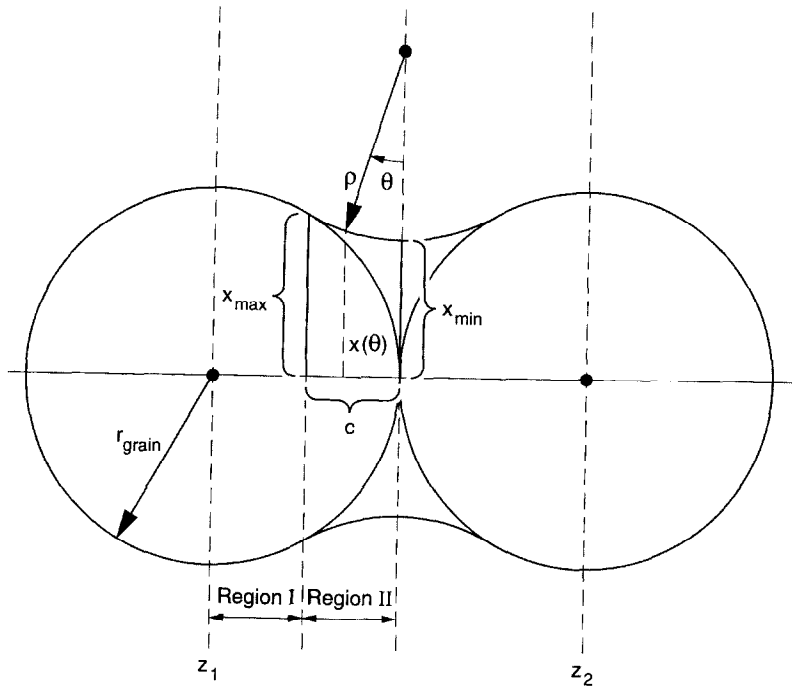


Fig. 1. Model of the intergranular bond.

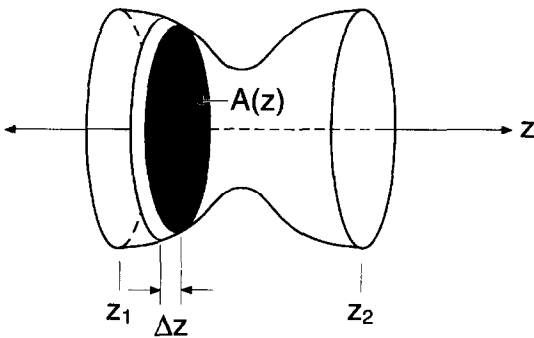


Fig. 2. Geometric quantities required for the calculation of the conductance of an individual bond.

$$R_2 = \frac{1}{k_{ice}\pi\rho} \int_{\sin^{-1}(\frac{r_{grain}}{r_{grain}+\rho})}^0 \frac{\cos\theta d\theta}{[x(\theta) + \rho(1 - \cos\theta)]^2} \tag{7}$$

where  $\rho$  is the external radius of curvature,  $x(\theta)$  is the internal radius of the bond in a plane perpendicular to the bond axis, and  $\theta$  sweeps from the intersection of the spherical and paraboloid regions to the center of the bond. The bond conductance is then computed as

$$g(r_{grain}, x_{min}) = \frac{1}{2[R_1(r_{grain}, x_{min}) + R_2(r_{grain}, x_{min})]} \tag{8}$$

In snow,  $g$  for any given bond changes with time and snow type and is the fundamental element of heat conduction in the grain lattice. The first step in this EMA is that snow will be treated as a population of thermal conductors whose values follow a particular frequency distribution  $[G(g)]$  that gives the average conductance  $g_m$ .

For a given relative bond radius,  $x_{min}/r_{grain}$ , the conductance of the bond is approximately proportional to the grain radius (Fig. 3), since the contact area between grains increases with grain size, but the length of the conductor in our model increases as  $2r_{grain}$ . For a given grain radius, the dependence of  $g$  on  $x_{min}/r_{grain}$  is also surprising (Fig. 4). For small relative bond sizes, the dependence is strong. The slope of  $g$  vs  $x_{min}/r_{grain}$  then decreases for moderate values of  $x_{min}/r_{grain}$  and it increases slightly as the bond approaches a cylindrical shape ( $x_{min}/r_{grain} = 1$ ). This behavior suggests that when bonds are growing initially, we should expect conductances to change more rapidly than when they are more mature. This agrees qualitatively with our observations and theories of a range of snow properties.

This model can calculate exactly the conductivity of a lattice constructed of such bonds in any arbitrary configuration. However, in snow, as in most aggregate materials, the bonds are not of uniform conductance. A statistical approximation could be made by directly estimating the probability density function of bond conductances. While we have no physically reasonable way to estimate such a distribution, we do have some evidence that grain sizes in snow are distributed log-

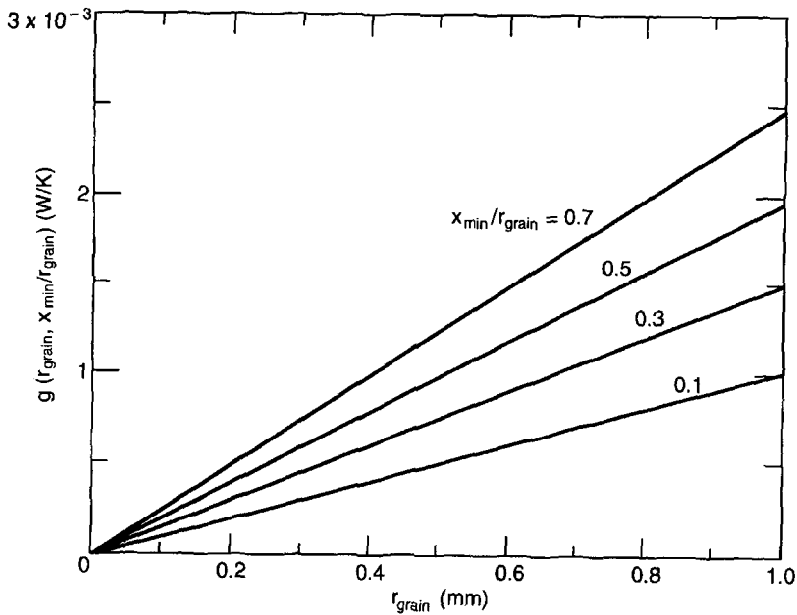


Fig. 3. Bond conductance vs grain radius  $r_{\text{grain}}$  with the relative bond radius  $x_{\text{min}}/r_{\text{grain}}$  as a parameter.

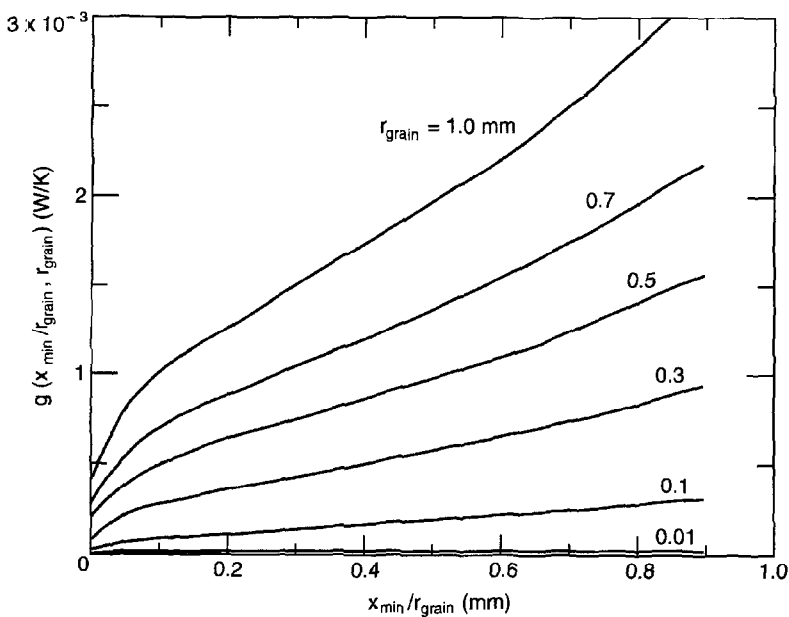


Fig. 4. Bond conductance vs  $x_{\text{min}}/r_{\text{grain}}$  with  $r_{\text{grain}}$  as a parameter. In the initial stages of formation, bonds between larger grains gain conductance so much more rapidly than those between smaller grains that when plotted on the same scale, it appears that they have finite conductance when the relative neck radius is zero. In reality, when  $x_{\text{min}}/r_{\text{grain}}$  goes to zero  $g$  converges to zero for all values of  $r_{\text{grain}}$ .

normally as are the particles in many aggregate systems [20]. A lognormal distribution has been observed directly in wet snow by Colbeck [21]. Therefore, we derive a probability density function,  $G(g)$ , for bond conductances by assuming that  $r_{\text{grain}}$  is distributed lognormally and by using the observation that bond growth is limited by the smaller grain. Thus,  $G(g)$

represents a population of bond conductances that constitutes the thermal conduction network and whose parameters are related to observable physical properties.

$G(g)$  is derived by fixing the relative bond radius. This implies that everywhere in the modeled snow, bond radii have grown to the same fraction of the

radii of the grains they join. Then, bond conductance depends only on the variable  $r_{\text{grain}}$ , with metamorphic state, represented by  $x_{\text{min}}/r_{\text{grain}}$ , as a parameter. Thus,

$$g = g(r_{\text{grain}})|_{x_{\text{min}}/r_{\text{grain}}} \quad (9)$$

Assuming  $r_{\text{grain}}$  is lognormally distributed:

$$f(r_{\text{grain}}) = \frac{1}{r_{\text{grain}} \sqrt{2\pi} \ln(\sigma)} \exp \left\{ - \left[ \frac{\ln(r_{\text{grain}}/\eta)}{\sqrt{2} \ln \sigma} \right]^2 \right\} \quad (10)$$

where  $\eta$  and  $\sigma$  are the mean and standard deviation of the distribution, respectively. In order to obtain the probability density function of conductances,  $G(g)$ , we need to know the functional form of equation (9), which is reasonably approximated as:

$$g \cong M \cdot r_{\text{grain}} \quad (11)$$

$M$  depends on the relative neck radius  $x_{\text{min}}/r_{\text{grain}}$  (Fig. 3). Following DeGroot ([22], p. 153), the probability distribution function  $G(g)$  is then given by

$$G(g) = f[r_{\text{grain}}(g)] \left| \frac{dr_{\text{grain}}}{dg} \right| \quad (12)$$

Using equation (11),

$$r_{\text{grain}}(g) \cong \frac{g}{M} \quad (13)$$

and inserting equations (10) and (13) into equation (12), we obtain

$$G(g) \cong \frac{1}{g \sqrt{2\pi} \ln(\sigma)} \exp \left\{ - \left[ \frac{\ln \left( \frac{g}{M\eta} \right)}{\sqrt{2} \ln(\sigma)} \right]^2 \right\} \quad (14)$$

which is nearly lognormal.  $\eta$  and  $\sigma$  are the parameters of  $f(r_{\text{grain}})$ . Now, the first averaging step of the EMA is employed to obtain  $g_m$ , defined as the solution of equation (2).

### CONDUCTOR CONNECTIVITY

In previous modeling efforts in snow physics, little progress has been made to explicitly determine the value or the significance of the coordination number. Adams and Sato [4] used an empirical relationship between coordination number and ice volume fraction that we express in terms of snow density,  $\rho_s$  ( $\text{g cm}^{-3}$ ):

$$\zeta = 3.565 - 8.108\rho_s + 29.52\rho_s^2 \quad (15)$$

Ridgway and Tarbuck [23] obtained an empirical relationship between void fraction and coordination number for 'random packings' of spheres. Later, Dullien [24] asserted that this relationship also holds for a wide variety of regular and random aggregates. For snow, it is:

$$\rho_s = -0.066 + 0.109\zeta - 0.004\zeta^2 \quad (16)$$

These relationships must be used with caution since they give unreasonable values of coordination number in the limit  $\rho_s \rightarrow 0$ . Ridgway and Tarbuck also give the void fraction for the most regular packing possible for uniform spheres at any coordination number. We show this in terms of snow density along with the empirical relationships (Fig. 5).

### ACCOUNTING FOR NETWORK GEOMETRY: THE $t$ -factor

The next step toward determining  $K_{\text{lat}}$  is to estimate the  $t$ -factor in equation (3). The summation in (3) includes all of the bonds that pass through a plane of area  $A_p$ , which is normal to the constant, one-dimensional, macroscopic temperature gradient,  $T'$ . In general, the summation divided by  $A_p$  represents a discrete averaging process that conceptually homogenizes the heterogeneous material over a region. Ideally, we would use a three-dimensional reconstruction to calculate the  $t$ -factor directly from serial photomicrographs of an actual snow sample, but such techniques are still under development. Thus, we used the common assumptions that grains are spherical and are arranged on a cubic lattice (Fig. 6) to evaluate the  $t$ -factor. The density of such a lattice, about  $480 \text{ kg m}^{-3}$ , is within the range of dense snow. An ideal lattice of this type has a coordination number of six. Equation (3) requires that we calculate the sum of the components of all bonds passing through a plane that is perpendicular to the average temperature gradient. For the face-centered cubic lattice, a unit cell has area  $A_p$ , normal to the temperature gradient, given by

$$A_p = (2\eta)^2 \quad (17)$$

in which  $\eta$  is the mean grain radius.

Aggregates with true face-centered cubic (fcc) structure have coordination number six, and the empirical equations (15) and (16) show that real aggregates exhibit a similar relationship between density and coordination number when corrections are made for specific gravity. Later, we treat snow as a cubic aggregate with coordination number six, but experience suggests that this is an overestimate. Rapid bond growth between snow grains during the settling process and the formation of necks in the needle-shaped particles interfere with the packing process and generates a large number of grains with a small number of bonds. This lowers the average coordination number.

Quantitative study of snow coordination number is lacking, so we estimate maximum and minimum values for  $k_{\text{lat}}$  using the bounding  $t$ -factor values based on coordination numbers six and three, respectively. The maximum value arises in a straightforward manner by including all six bonds for each grain in the fcc model. The minimum requires that we treat the aggregate as if it were packed as an fcc structure with

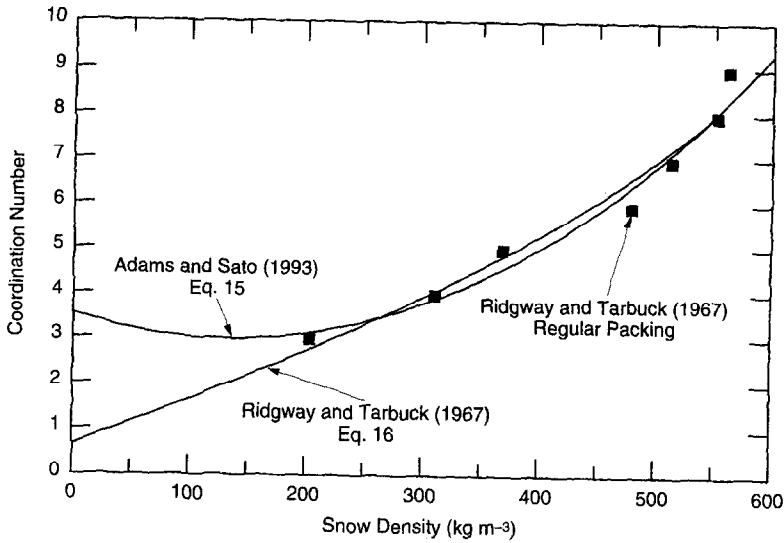


Fig. 5. Two empirical approximations of coordination number as a function of aggregate density compared to calculations using systematic packing.

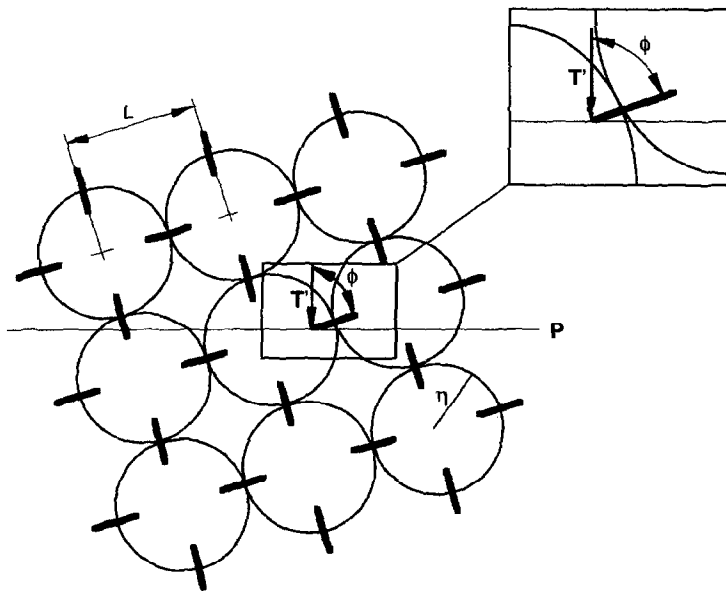


Fig. 6. Model for determination of *t*-factor. Bold line segments schematically indicate locations of intergranular bond axes, but their geometries are defined as in Figs. 1 and 2. Bonds perpendicular to the plane of the diagram are not shown. The *t*-factor is calculated over a representative area  $A_p$  in plane  $P$ , perpendicular to temperature gradient.

some intergranular bonds missing. As such, we apply the coordination number in a simple stochastic manner to the *t*-factor by assuming that each bond has only a 3/6 probability of being present in the grain lattice.

Finally, we note that  $A_p$  has an implicit cosine dependence that renders the *t*-factor independent of  $\phi$  when the cubic structure is rotated, and the term is given by

$$t\text{-factor} = \frac{1}{2\eta} \tag{18a}$$

when the snow has maximal connectivity and

$$t\text{-factor} = \frac{3}{6} \frac{1}{2\eta} \tag{18b}$$

when it has minimal connectivity. This would correspond to densities of 480 and 225 kg m<sup>-3</sup>, respec-

tively, following Fig. 5. The relationship between density and coordination number when density is  $225 \text{ kg m}^{-3}$  is not based on fcc structure with missing bonds, but we have made this assumption to isolate the effects of coordination number and to aid in determining a lower bound for  $k_{\text{lat}}$  that is geometrically consistent with its upper bound.

### TIME DEPENDENCE: EFFECT OF SINTERING

The geometric instability of snow is well-known, and it is this characteristic that gives rise to the need for a model that shows how thermal conductivity changes in response to metamorphism. Where two grains come into contact, sintering causes substantial bonds to form between them as a result of mass diffusion into the region of the contact area. We use the gaseous diffusion model of Hobbs and Mason [25], which is based on bond neck size,  $x_{\text{min}}/r_{\text{grain}}$ , time,  $t$ , and temperature,  $T$ :

$$\left(\frac{x_{\text{min}}}{r_{\text{grain}}}\right) = \frac{B(T)}{r_{\text{grain}}^3} t \quad (19)$$

where  $B(T)$  is a function of temperature and physical constants:

$$B(T) = \frac{20\gamma\delta^3}{k_b T} \left[ \frac{k_b T\beta}{p_o m D_g} + \frac{L_s^2 m \rho_{\text{ice}}}{k_{\text{air}} k_b T^2} \right]^{-1}. \quad (20)$$

Although their sintering model only qualitatively agrees with the measurements of bond radius growth they obtained, we used it because we desired a general physically based model and, for ice, this one has not yet been superseded. Since our EMA model is general, future modifications of the sintering model would be easily incorporated. Therefore, we used the Hobbs and Mason [25] model to investigate the dependence of bond conductance on time, which constrains  $\rho$  in equation (7) and allows  $g$  to be calculated using (8). For a given elapsed time, the dependence of  $g$  on  $r_{\text{grain}}$  is virtually linear (Fig. 7) and, while it is common to observe relative bond radii as large as about 0.7, that is the upper limit of what we consider. From this, bond conductance is shown as a function of time with  $r_{\text{grain}}$  as a parameter in Fig. 8.

To apply the network approximation to a time-varying lognormal distribution of grains, it is necessary to find the time-dependent functional dependence of  $g$  on  $r_{\text{grain}}$  in analogy with equation (11). The results in Fig. 7 indicate that a linear curve fit is appropriate ( $r_{\text{min}}^2 = 0.996$ ). At any time, then, the functional dependence of  $g$  on  $r_{\text{grain}}$  will be defined by the values of slope  $M$  and intercept  $b$ ,

$$g(r_{\text{grain}}, t) \cong M(t) \cdot r_{\text{grain}} + b(t). \quad (21)$$

The time dependences of  $M$  and  $b$  may themselves be approximated by polynomials that depend on temperature. Then the probability density function for

bond conductance for a given time may be derived in the same manner as in the time-dependent case. Equations (13) and (14) become, for a given temperature,

$$r_{\text{grain}}(g, t) \cong \frac{g - b(t)}{M(t)} \quad (22)$$

and

$$G(g, t) \cong \frac{1}{[g - b(t)]\sqrt{2\pi \ln(\sigma)}} \exp \left\{ - \left[ \frac{\ln \left( \frac{g - b(t)}{\eta \cdot M(t)} \right)}{\sqrt{2 \ln(\sigma)}} \right]^2 \right\}. \quad (23)$$

Equations (22) and (23) have been evaluated using a mean grain size of 0.2 mm, a standard deviation of 1.2, and four values of  $t$  that span the early stages of development of a dry snow cover (Fig. 9). As the snow matures and the population of conduction elements becomes more conducting, the dispersion increases because the product  $\eta M$  grows; the details of this effect will be different for different choices of growth models and particle size distributions. Furthermore, no model of the temporal evolution of the grain size distribution exists for dry snow, but if such a model were available, we could easily include it in equation (23).

### MICROSTRUCTURAL CONTROL OF $K_{\text{lat}}$ THROUGH NETWORK ATTRIBUTES: ANALYSIS OF $g_m$

In our model, mean grain radius,  $\eta$ , geometric standard deviation of grain radius,  $\sigma$ , average coordination number,  $\bar{\zeta}$ , and time,  $t$ , govern ensemble average conductance,  $g_m$ . In most cases,  $g_m$  increases as each one of these parameters increases. For example, larger grains enhance heat transfer across individual bonds and thus cause the  $g_m$  to increase. Indeed,  $g_m$  is generally most sensitive to  $\eta$ . Also, as  $\bar{\zeta}$  increases, there are more pathways available for heat conduction, so  $g_m$  also increases.

There are also interactions among the microstructural quantities that have important effects. Observers have noted that in many systems whose constituents have properties that depend on log-normally distributed particles, a small number of very large particles from the tail of the distribution can have a controlling influence on the macroscopic behavior of the system. We also observed this behavior in our model, but only when the coordination number is large. When the coordination number is small, it is the low-valued end of the distribution that limits heat conduction. Our interpretation is that when the network is poorly connected (small coordination number), highly conductive pathways are unable to dominate heat flow because they are isolated from each other. On the other hand, when



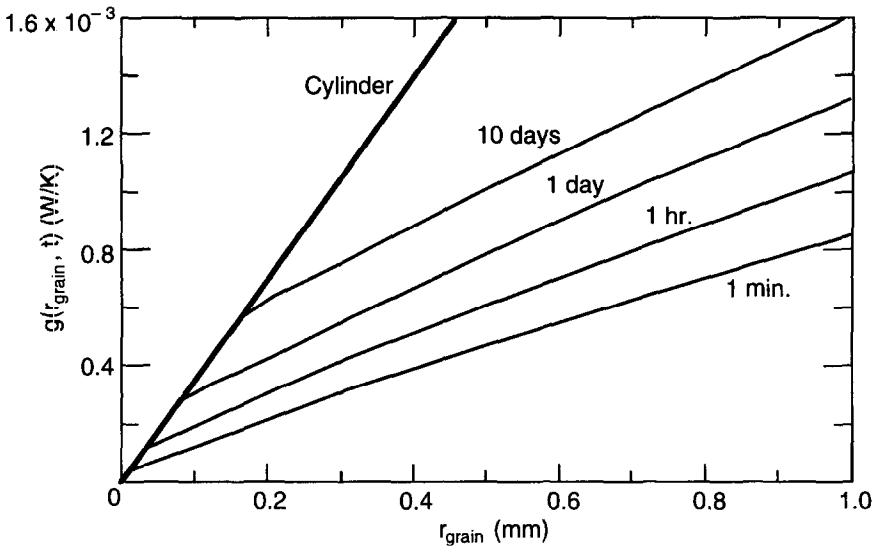


Fig. 7. Bond conductance vs  $r_{\text{grain}}$  at four different times after the grains are brought into contact. We truncate the bond growth at the cylindrical limit.

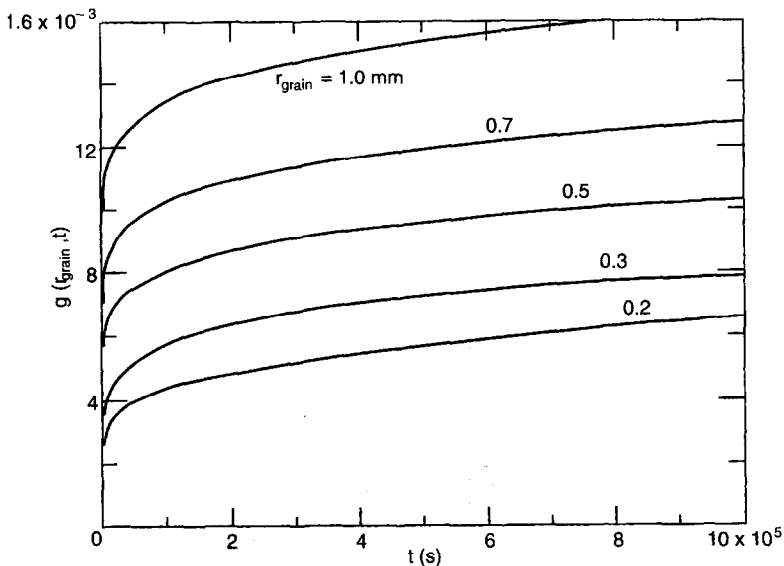


Fig. 8. Bond conductance vs time with  $r_{\text{grain}}$  as a parameter.

individual conductors are more likely to be interconnected as in the case of a large coordination number, even a few highly conductive pathways can have a strong effect on the overall conductivity of the system because heat can by-pass highly resistive pathways.

Figures 10 and 11 show  $g_m$  as a function of  $\eta$  and  $\sigma$  at four times and two values of  $\zeta$ . Note that  $\partial g_m / \partial \sigma$  is most positive for high connectivity and well-developed bonds, while it is most negative when connectivity is low, bonds are young, and grains are large. This reflects the connectivity-limited heat flow

through the network and the influence of poorly conducting bonds when connectivity is small. The sensitivity to poorly conducting bonds seems to be greatest when connectivity and bond growth are small and when grains are large.

When grains are large, they offer less resistance to heat flow and allow the flow-limiting effects of coordination number to dominate. It is important to recognize that in drawing this conclusion, we are making use of the model to separate the effects of the population of bonds from the effects of the aggregate as a whole. For example, for a given relative neck

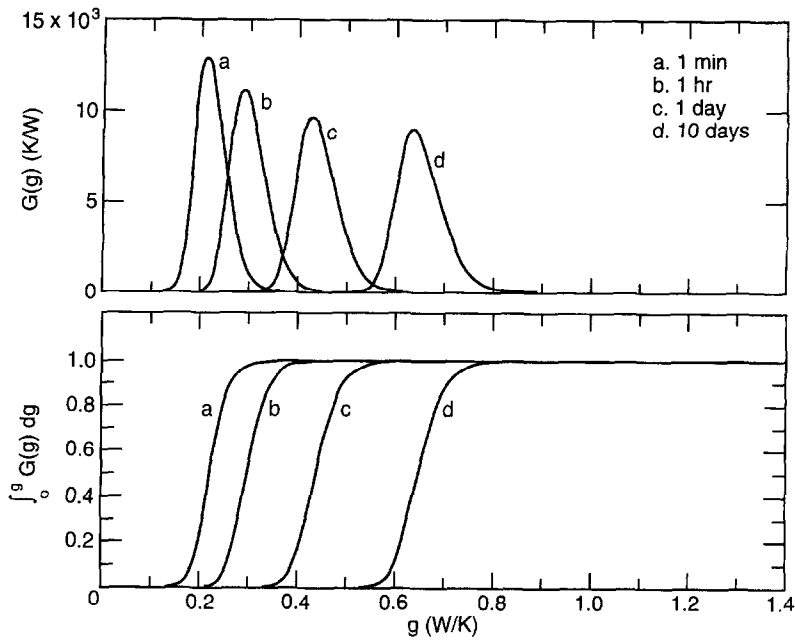


Fig. 9. (top) Probability density function of conductances at four times; (bottom) probability function of conductances at four times. Mean grain size,  $\eta$ , and standard deviation,  $\sigma$  (dimensionless), are 0.2 mm and 1.2, respectively, for all curves.

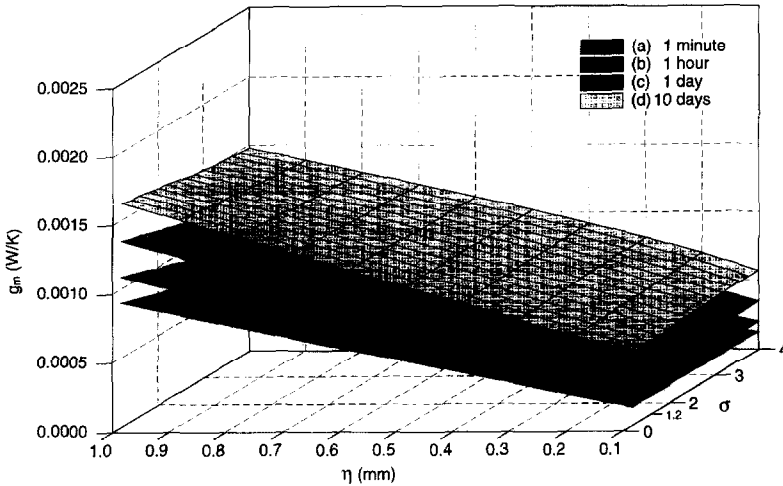


Fig. 10.  $g_m$  vs  $\eta$  and  $\sigma$  with average coordination number of 2.5.

radius, heat flow through a bond will increase as grain size increases. As we expect,  $\partial g_m / \partial \eta$  is always positive and is greatest when  $t$  and  $\sigma$  are large. This analysis of  $g_m$  shows the importance of the grain size effect relative to the effects of network connectivity. In contrast, when we examine the behavior of the macroscopic system using the  $t$ -factor, we will see that the macroscopic conductivity *decreases* with increasing grain size.

**CONDUCTIVITY OF SENSIBLE HEAT THROUGH THE AGGREGATE: THE ROLE OF THE  $t$ -FACTOR**

Calculated values of  $K_{lat}$  (Figs. 12 and 13) bound the expected values of the thermal conductivity of the ice grain lattice of snow [1, 17]. Figure 12 shows the upper limit calculated from the fcc-structured model and Fig. 13 shows the lower limit using the simple stochastic modification of that model discussed above.

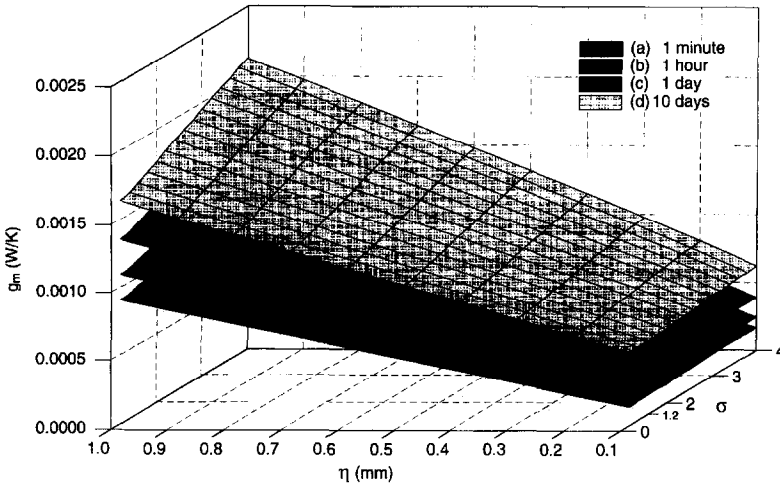


Fig. 11.  $g_m$  vs  $\eta$  and  $\sigma$  with average coordination number of six.

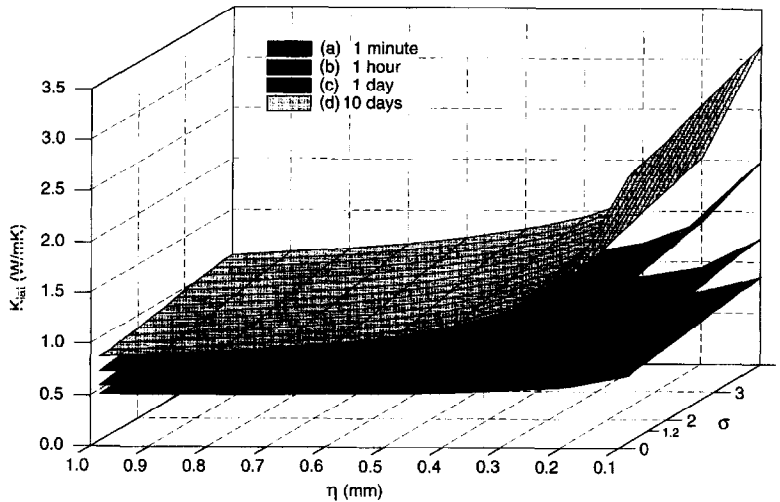


Fig. 12.  $K_{lat}$  vs  $\eta$  and  $\sigma$  with average coordination number of six.

Both show the same general dependences on intergranular bond development and grain size distribution parameters.

In the maximum estimations of Fig. 12, estimates for the most mature stage of development (10d) reach and exceed the thermal conductivity of solid ice. While fully mature snow is expected to contain well-developed bonds, these are clearly overestimates of  $K_{lat}$  since the bonds would not produce a network that behaves like solid ice. These high values reflect the cautious estimate of the coordination number and show our limited ability to estimate the  $t$ -factor. More realistic estimates of the coordination number and the  $t$ -factor are required, and these should bring the estimated maximum values of  $K_{lat}$  more in line with published data and increase confidence that the range reported here accurately bounds actual values. Unfor-

tunately, such estimates appear to be beyond the reach of analytic geometry and will have to wait for the development of better numerical and microscopic techniques.

The most salient feature of the estimates of  $K_{lat}$  is that the  $1/\eta$  dependence introduced by the  $t$ -factor as we modeled it gives a counterintuitive dependence of  $K_{lat}$  on mean grain size. Clearly, though, as the grains become larger, the number of bonds per unit volume must decrease; while  $g_m$  increases with increasing  $\eta$ , the  $t$ -factor decreases faster. To support this interpretation, more advanced quantitative microscopic techniques coupled with careful laboratory measurements will be required. We interpret the dependence of  $K_{lat}$  on  $\sigma$  as a direct expression of the interplay between conductance distribution and coordination number that controls  $g_m$ .

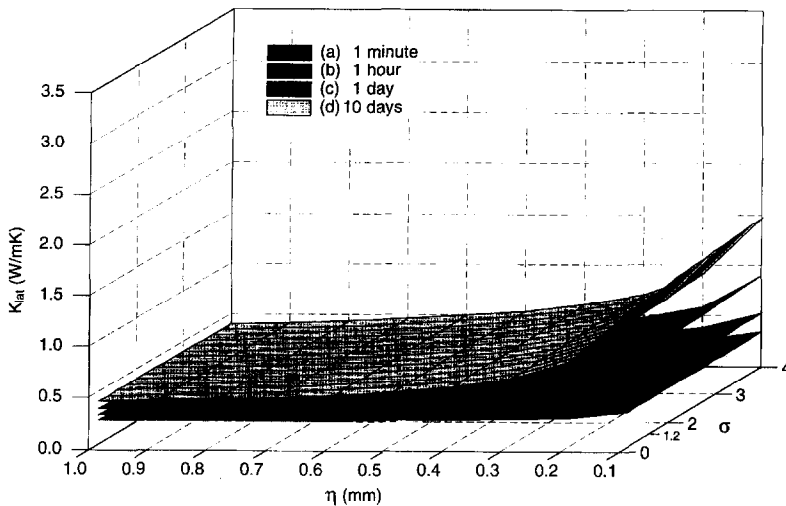


Fig. 13.  $K_{lat}$  vs  $\eta$  and  $\sigma$  with average coordination number of three.

## DISCUSSION

This model is a starting point for understanding the variation of thermal conductivity with snow type and at the boundaries of a snow layer, where textural gradients are commonly observed but still difficult to quantify. It requires more knowledge about the characteristics of snow grains and interconnectedness than models that preceded it. In exchange for the additional challenge of using the model, it can incorporate information in a physically meaningful way. We obtained reasonable physically based approximations for the lattice thermal conductivities of rounded, dense, dry snow in the absence of multigrain structures. Arons [17] showed that the approach can easily accommodate multigrain structures, as long as conductance pathways are defined as statistically independent with respect to heat flow. Sturm *et al.* [3] showed that thermal conductivity of snow containing multigrain structures is less sensitive to changes in density than snow without such structures, and Arons [17] found that sensible heat flow in the former was sensitive to the length of the structures.

Freshly fallen snow could also be treated, but care would be required to interpret the meaning of 'conduction element' in a network that is partly composed of dendritic particles. Developing an analytical expression for the  $t$ -factor that applies to snow of lower density that preserves a sense of physically realistic quantitative geometry will be challenging. Estimating this quantity requires knowledge of bond length, orientation, and volumetric concentration, which makes it sensitive to changes in snow type. Therefore, a method to estimate the  $t$ -factor directly should be developed using photomicrographs as per Arons *et al.* [26].

We used the semiempirical sintering model developed by Hobbs and Mason [25] to investigate changes in thermal conductivity due to sintering, but

disagreement between their model and their data suggest that we are still a long way from understanding the details of sintering between pairs of ice bodies. We are even further from a compelling model for sintering in multiparticle aggregates. Knowledge of sintering must be developed if we are to gain further understanding of the time dependence of  $K_{lat}$  or other important physical properties.

Another important extension of the theory presented here will be the treatment of latent heat flow. Although sensible heat accounts for at least half of the heat flow in snow, latent heat transfer can be as important at high temperatures. When vapor transport is significant, local temperature gradient enhancement [27] introduces a nonlinearity that prohibits the direct application of EMA to the vapor component of heat transfer in dry snow. The vapor flow component of the overall conductivity could possibly be linearized and introduced as a subpopulation of conductance values. However, at present, we are restricted to studying only heat flow through the ice grain lattice using the EMA. Nonetheless, understanding the characteristics of heat flow through the grain lattice will likely lead to a greater understanding of the water vapor contribution as well.

## CONCLUSIONS

Changes in snow microstructure cause changes in its thermal conductivity. This model allows us to understand how the conduction of sensible heat in snow depends on microstructural characteristics that are well-defined, physically meaningful, and, in principle, measurable. We know that the thermal conductivity of snow depends on the meteorological conditions that prevailed during its deposition and on the thermal and mechanical processes that act on it thereafter. We can now quantify how the conduction

of sensible heat in snow is governed by the characteristics that are sensitive to meteorological and thermal history. They include grain bond geometry, grain size distribution, coordination number, bond orientation, bond concentration, temperature, and time. By extension, one may also demonstrate the dependence on temperature gradient through the development of multigrain structures.

We modeled the bonds in snow as statistically independent quasi-linear conductors between pairs of grains. The conductance of each bond was calculated directly. We expected this conductance to increase quadratically with relative neck size,  $x_{\min}/r_{\text{grain}}$ , as it would for a cylindrical object, but we found a more complicated relationship. Conductance increases rapidly with relative neck size at first, then slows for moderate values of  $x_{\min}/r_{\text{grain}}$ , and accelerates again as  $x_{\min}/r_{\text{grain}}$  approaches one. This is independent of the kinetics of sintering and shows the need for careful modeling of heat transfer and other bond-dependent properties in snow when the material is undergoing metamorphism.

We determined an ensemble mean conductance value for the population of bonds using concepts from random resistance network theory. This average is usually controlled by the mean of the conductance distribution, but it also depends on the average coordination number of the ice grain network. The low-conductance tail of the probability density function of bond conductances is responsible for limiting heat flow when connectivity is low. This effect is stronger when the mean of the conductance distribution is higher and the low-conductance tail is thus longer. These new insights help explain the results of previous qualitative investigations of parallel and serial heat flow through snow and other aggregates. We also showed how the ensemble mean conductance changes as the metamorphic process of sintering evolves. Our ability to model sintering in snow and other aggregates is limited, but there is no doubt that the process is critical for the evolution of thermal conductivity and other properties in snow. The present model demonstrates how its effects can be inductively included.

We then used the  $t$ -factor to show that while the ensemble mean *conductance* increases with increasing grain size, the macroscopic *conductivity* decreases as grains become larger and force the intergranular bond density to decrease. Estimates of the  $t$ -factor are more compelling for high density snow than for low density snow, because of packing irregularities at low density. Improved estimates of the  $t$ -factor for low density snow will require the application of emerging numerical and micrographic techniques. In general, such techniques should enable us to calculate the necessary statistics of bond conductances, orientations, and coordination numbers, and will improve our knowledge of both  $g_m$  and the  $t$ -factor.

The power of the effective medium approximation for conductivity of sensible heat in snow lies in its physical foundation and versatility. We are now able

to explain the control of heat flow through the ice grain lattice of snow by geometric attributes that can be observed in nature. In principle, the effective medium approximation can be applied to a variety of different snow types and meteorological conditions that are important in cold regions.

*Acknowledgments*—This work was conducted under CRREL project Physical Properties of Snow Covers, AT24-5C-501. We thank Kathy Jones, Joel Koplik, Bert Davis, and Matthew Sturm for useful technical discussions.

## REFERENCES

1. Arons, E. M. and S. C. Colbeck, Geometry of heat and mass transfer in dry snow: a review of theory and measurement. *Reviews of Geophys.*, 1995, **33**, 463–493.
2. Torquato, S., Random heterogeneous media: microstructure and improved bounds on effective properties. *Applied Mechanics Review*, 1991, **44**, 37–76.
3. Sturm, M., Holmgren, J., König, M. and Morris, K., The thermal conductivity of seasonal snow. *Journal of Glaciology*, 1997, **43**, 26–41.
4. Adams, E. E. and Sato, A., Model for effective thermal conductivity of a dry snow cover composed of uniform ice spheres. *Annals of Glaciology*, 1993, **18**, 300–304.
5. Shabtaie, S. and Bentley, C. R., Unified theory of electrical conduction in firm and ice: site percolation and conduction in snow and firm. *Journal of Geophysical Research*, 1994, **99**, 19 757–19 769.
6. Kossacki, K. J., Komle, N. I., Kargl, G. and Steiner, G., The influence of grain sintering on the thermoconductivity of porous ice. *Planetary and Space Science*, 1994, **42**(5), 383–389.
7. Watanabe, Z., Proposition of a net-like model of snow. *Annals of Glaciology*, 1993, **18**, 72–78.
8. Shante, V. K. and Kirkpatrick, S., An introduction to percolation theory. *Advances in Physics*, 1971, **20**, 325–357.
9. Koplik, J., Homogenization and effective medium methods for transport in disordered granular systems. In *Physics of Granular Media*, ed. D. Bideau and J. A. Dodds. Nova, NY, 1991, pp. 215–234.
10. Kirkpatrick, S., Percolation and conduction. *Reviews of Modern Physics*, 1973, **45**, 574–588.
11. Koplik, J., Lin, C. and Vermette, M., Conductivity and permeability from microgeometry. *Journal of Applied Physics*, 1984, **56**, 3127–3131.
12. Koplik, J., On the effective medium theory of random linear networks. *Journal of Physics C: Solid State Physics*, 1981, **14**, 4821–4837.
13. Colbeck, S. C., Snow metamorphism and classification. In *Seasonal Snowcovers: Physics, Chemistry, Hydrology*, ed. H. G. Jones and W. J. Orville-Thomas. D. Reidel Publishing Company, Dordrecht, 1987, pp. 1–35.
14. Colbeck, S., Akitaya, E., Armstrong, R., Gubler, H., Lafeuille, J., Lied, K., McClung, D. and Morris, E., *The International Classification for Seasonal Snow on the Ground*. The International Commission on Snow and Ice of the International Association of Scientific Hydrology (available from World Data Center, University of Colorado, Boulder CO), 1990.
15. Pitman, D. and Zuckerman, B., Effective thermal conductivity of snow at  $-88$ ,  $-27$ , and  $-5^{\circ}\text{C}$ . *Journal of Applied Physics*, 1967, **38**, 2698–2699.
16. Sturm, M. and Johnson, J. B., Thermal conductivity measurements of depth hoar. *Journal of Geophysical Research*, 1992, **97**, 2129–2139.

17. Arons, E. M., Dependence of snow thermal conductivity on microstructure, Ph.D. thesis, Dartmouth Coll., Hanover, NH, 1994.
18. Halliday, D. and Resnick, R., *Fundamentals of Physics*, 2nd edn. John Wiley and Sons, New York, 1981, p. 816.
19. Kuczynski, G. C., Self-diffusion in sintering of metallic particles. *Journal of Metals*, 1949, **1**, 169–178.
20. Irani, R. R. and Callis, C. F., *Particle Size: Measurement, Interpretation, and Application*. John Wiley and Sons, New York, 1963, p. 165.
21. Colbeck, S. C., Statistics of coarsening in water-saturated snow. *Acta Metallurgica*, 1986, **34**, 347–352.
22. DeGroot, M. H., *Probability and Statistics*, 2nd edn. Addison-Wesley Publishing Co., Reading, MA, 1986.
23. Ridgway, K. and Tarbuck, K. J., The random packing of spheres. *British Chemical Engineering*, 1967, **12**, 384–388, 1967.
24. Dullien, F. A. L., *Porous Media: Fluid Transport and Pore Structure*, 2nd edn. Academic Press, San Diego, 1992.
25. Hobbs, P. V. and Mason, B. J., The sintering and adhesion of ice. *Philosophical Magazine*, 1964, **9**, 181–197.
26. Arons, E. M., Davis, R. E. and Kwiecien, M. J., Numerical reconstruction of snow microstructure and mesostructure (abstract). *Eos Trans. AGU, Fall Meet. Suppl.*, 1995, **76**(46), 184.
27. Colbeck, S. C., Theory of metamorphism of dry snow. *Journal of Geophysical Research*, 1983, **88**, 5475–5482.